Coherence Properties and Quantum State Transportation in an Optical Conveyor Belt

S. Kuhr,* W. Alt, D. Schrader, I. Dotsenko, Y. Miroshnychenko, W. Rosenfeld, M. Khudaverdyan, V. Gomer, A. Rauschenbeutel, and D. Meschede

Institut für Angewandte Physik, Universität Bonn, Wegelerstrasse 8, D-53115 Bonn, Germany

(Received 11 April 2003; published 19 November 2003)

We have prepared and detected quantum coherences of trapped cesium atoms with long dephasing times. Controlled transport by an ''optical conveyor belt'' over macroscopic distances preserves the atomic coherence with slight reduction of coherence time. The limiting dephasing effects are experimentally identified, and we present an analytical model of the reversible and irreversible dephasing mechanisms. Our experimental methods are applicable at the single-atom level. Coherent quantum bit operations along with quantum state transport open the route towards a ''quantum shift register'' of individual neutral atoms.

DOI: 10.1103/PhysRevLett.91.213002 PACS numbers: 32.80.Lg, 32.80.Pj, 42.50.Vk

Obtaining full control of all internal and external degrees of freedom of individual microscopic particles is the goal of intense experimental efforts. The long lived internal states of ions and neutral atoms are excellent candidates for quantum bits (qubits), in which information is stored in a coherent superposition of two quantum states. Once sufficient control of individual particles is established, one of the most attractive perspectives is the engineered construction of quantum systems of two or more particles. Their coherent interaction is a key element for the realization of quantum gates and can be implemented by transporting selected qubits into an interaction zone [1]. In this context, ions have successfully been transported between distinct locations while maintaining internal-state coherence [2].

In this Letter we report on the coherence properties and on a quantum state transportation of neutral atoms in a standing wave dipole trap. We present a scheme of preparation and detection of the electronic hyperfine ground states, which has been applied to ensembles as well as to single atoms. Along with the demonstration of 1-qubit rotations, our system is a promising candidate for storing quantum information, since the hyperfine ground states exhibit long ($\sim$200 ms) coherence times. In particular, the coherence even persists while transporting the atoms over macroscopic distances. This opens a route towards quantum gates via cavity-mediated atom-atom coupling.

We trap cesium atoms in a standing wave dipole trap ($\lambda = 1064$ nm) with a potential depth of $U_0 = 1$ mK, loaded from a high-gradient magneto-optical trap (MOT) [3,4]. The single-atom transfer efficiency between the two traps is better than 95% [5]. The MOT is also used to determine the exact number of trapped atoms by observing their fluorescence. By shifting the standing wave pattern along the direction of beam propagation, we can transport the atoms over millimeter-scale distances. This is realized by mutually detuning the frequencies of the dipole trap laser beams with acousto-optical modulators. Additionally, we use microwave radiation at $\omega_{\mathrm{hfs}}/2\pi = 9.2$ GHz to coherently drive the $|F = 4, m_F = 0\rangle \rightarrow |F = 3, m_F = 0\rangle$ clock transition of the $6\,^2S_{1/2}$ ground state with Rabi frequencies of $\Omega/2\pi = 10$ kHz.

The initial state is prepared by optically pumping the atom into $|F = 4, m_F = 0\rangle$. For this purpose, we use a π-polarized laser resonant with the $F = 4 \rightarrow F' = 4$ transition and a repumping laser on the $F = 3 \rightarrow F' = 4$ transition in a magnetic guiding field of $B = 100\ \mu$T. A state-selective detection method, which discriminates between the atomic hyperfine states, is implemented by exposing the atom to a σ^+-polarized laser, resonant with the $F = 4 \rightarrow F' = 5$ cycling transition. It pushes any atom in $F = 4$ out of the dipole trap, whereas an atom in $F = 3$ remains trapped. It is essential to push the atom in $F = 4$ out of the dipole trap before it spontaneously decays into $F = 3$ due to off-resonant excitation of the $F' = 4$ level. For this purpose, the dipole trap is adiabatically lowered to 0.1 mK before the push-out laser is shined in perpendicular to the trap axis with high intensity ($I/I_0 = 100$, where I_0 is the saturation intensity). In this regime the resonant radiation pressure force is stronger than the dipole force in the radial direction. We thus push the atom out of the trap within much less than a quarter of the radial oscillation period ($\sim$1 ms).

The number of atoms in $F = 3$ remaining in the dipole trap is determined by transferring them back into the MOT. In all experiments presented in this Letter we thus compare the number of atoms in the MOT before and after any coherent manipulation in the dipole trap. As a result of our state-selective detection process, about 1% of the atoms prepared in $F = 4$ survive the application of the push-out laser, whereas more than 95% of the atoms in the $F = 3$ state remain trapped. Note that, using this method, we have experimentally checked that we can securely detect the quantum state of a single atom [6].

The coherence time between the $|F = 4, m_F = 0\rangle$ and the $|F = 3, m_F = 0\rangle$ state is measured using Ramsey's method of separated oscillatory fields [7]. We describe the coherent evolution of the system by the semiclassical Bloch vector model [8]. The initial state $|F = 4, m_F = 0\rangle$ corresponds to the Bloch vector $(u, v, w) = (0, 0, -1)$.

The application of two $\pi/2$ pulses, separated by a time interval t, leads to the well-known Ramsey fringes $w(t) = \cos\delta t$, where $\delta = \omega - \omega_{\mathrm{hfs}}$ is the detuning of the microwave frequency ω from the atomic resonance ω_{hfs}. This leads to the theoretical population transfer to $F = 3$, $P_3(t) = [w(t) + 1]/2$. In the experiment, P_3 is measured using our state-selective detection method. We count the number of atoms in $F = 3$ and divide by the initial number of atoms in the MOT. Since the atoms are trapped in separate potential wells of the dipole trap and interactions between them can be neglected, we perform our experiments with about 50 atoms in order to reduce the measurement time. As there is no dependence on the number of atoms the ensemble results can be transferred to the single-atom case.

The observed Ramsey signal decays due to inhomogeneous broadening of the atomic resonance frequencies; see Fig. 1. This frequency spread arises from the energy distribution of the atoms in the dipole trap, which leads to a corresponding distribution of light shifts. For an atom in the bottom of a potential well (energy $E = 0$), the clock transition is light shifted by $\hbar\delta_0 = \eta U_0$, with $\eta = \omega_{\mathrm{hfs}}/\Delta = 1.45 \times 10^{-4}$ and $\delta_0 < 0$ [9]. Here, $\Delta/2\pi = -64$ THz is the effective detuning of the dipole trap laser,

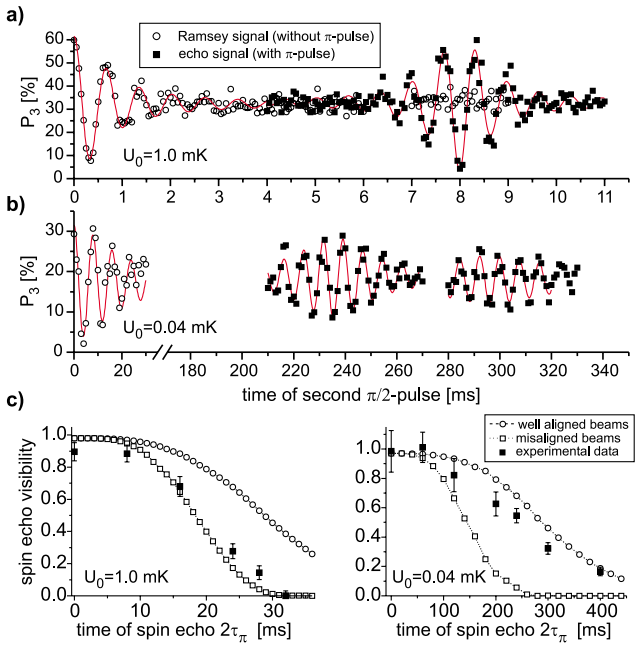

FIG. 1 (color online). Ramsey and spin echo signals. (a) $U_0 = 1.0$ mK. The application of a π pulse at $t = 4$ ms leads to a rephasing of the magnetic dipole moments at $t = 8$ ms (squares). The hollow circles show a Ramsey signal, obtained without a π pulse, but with otherwise identical parameters. Each point results from 30 shots with about 50 initial atoms. The lines are fits according to the analytic model presented in the text. (b) Ramsey signal and two different spin echoes for $U_0 = 0.04$ mK. (c) Decay of the spin echo visibility for different trap depths (filled squares) together with best (empty circles) and worst case predictions (empty squares).

taking into account contributions of the D_1 and the D_2 line. In a potential of $U_0 = 1$ mK this differential light shift is $\delta_0/2\pi = -3.0$ kHz. If the atom possesses an energy $E > 0$ in the trapping potential, the average light shift decreases to $\delta_{\mathrm{ls}}(E) = \delta_0 + \eta E/(2\hbar)$ in harmonic approximation. In our experiment, the energy distribution of the atoms has been measured to be a 3D Maxwell-Boltzmann distribution [10]. This results in a corresponding distribution of differential light shifts,

$$\tilde{\alpha}(\delta_{\mathrm{ls}}) = \frac{2K^{3/2}}{\sqrt{\pi}}\sqrt{\delta_{\mathrm{ls}} - \delta_0}\,\exp[-K(\delta_{\mathrm{ls}} - \delta_0)], \qquad (1)$$

with $K = 2\hbar/(\eta k_{\mathrm{B}} T)$, where T is the temperature of the atoms. From this distribution, we derive an analytic expression for the shape of the Ramsey signal. For an atom with light shift δ_{ls}, the w component of the Bloch vector, after application of the two $\pi/2$ pulses, is given by $w_{\mathrm{Ramsey}}(t) = \cos[(\delta + \delta_{\mathrm{ls}})t]$. Averaged over a thermal ensemble, the Ramsey signal is the integral over all light shifts, $w_{\mathrm{Ramsey,inh}}(t) = \int_{\delta_0}^{\infty} w_{\mathrm{Ramsey}}(t)\tilde{\alpha}(\delta_{\mathrm{ls}})d\delta_{\mathrm{ls}}$. The envelope of the Ramsey fringes is thus the Fourier cosine transform $\alpha(t)$ of the distribution of light shifts, yielding

$$w_{\mathrm{Ramsey,inh}}(t) = \alpha(t)\cos[(\delta + \delta_0)t], \qquad (2)$$

with

$$\alpha(t) = [1 + 2.79(t/T_2^*)^2]^{-3/4}. \qquad (3)$$

Despite this nonexponential decay, we have defined the inhomogeneous or reversible dephasing time $T_2^* = 1.67K$ as the $1/e$ time of the amplitude $\alpha(t)$.

The Ramsey fringes presented in Figs. 1(a) and 1(b) are fitted according to this model and yield $T_2^* = (0.86 \pm 0.05)$ ms and $T_2^* = (18.9 \pm 1.7)$ ms for $U_0 = 1.0$ mK and $U_0 = 0.04$ mK, respectively. The maximum value of P_3 of 60% in Fig. 1(a) includes imperfections in the optical pumping process (-20%) and atom losses caused by inelastic collisions during the transfer from the MOT into the dipole trap (-20%). The additional reduction to 30% in Fig. 1(b) occurs during the lowering of the trap, where hot atoms are lost. Note that the coherence is not impaired by these losses as the maximum visibility is close to 100% (see Fig. 1).

The inhomogeneous dephasing can be reversed by applying a π pulse between the $\pi/2$ pulses, in analogy to the spin-echo technique in nuclear magnetic resonance [11]. In optical dipole traps, this technique was recently employed by another group [12], independently of our work. Our spin-echo signals are presented in Figs. 1(a) and 1(b), showing that the inhomogeneous dephasing can be reversed almost completely. In the low dipole trap [Fig. 1(b)] we observe a pronounced spin echo even for pulse delays of up to $2\tau_\pi = 300$ ms, where τ_π denotes the time of the π pulse. Similar to the Ramsey fringes, the shape of the echo signal is $w_{\mathrm{echo}}(t) = -\alpha(t - 2\tau_\pi)\cos[(\delta + \delta_0)(t - 2\tau_\pi)]$.

In Fig. 1(c) we plot the visibility of the echo signals as a function of $2\tau_\pi$ for the two trap depths. The decay is due to an irreversible dephasing of the atomic coherence with a time constant T_2', defined as the $1/e$ decay time of the spin-echo visibility. For the two trap depths, of $U_0 = 1.0$ mK and $U_0 = 0.04$ mK, we obtain $T_2' = 10.2 \pm 0.4$ ms and $T_2' = 146 \pm 7$ ms, respectively. To account for the irreversible dephasing, we extend our model to the case of a time-varying detuning, $\delta(t)$, in order to account for a variation of the precession angles of the Bloch vector, $\phi_1 = \int_0^{\tau_\pi} \delta(t)dt$ and $\phi_2 = \int_{\tau_\pi}^{2\tau_\pi} \delta(t)dt$, before and after the π pulse. The phase difference $\phi_2 - \phi_1$ is expressed as a difference of the detuning, $\Delta\delta$, averaged over τ_π. The w component of the Bloch vector at $t = 2\tau_\pi$ then reads $w_{\text{echo}}(\Delta\delta, 2\tau_\pi) = -\cos(\Delta\delta\,\tau_\pi)$. In the following considerations, we assume that all atoms experience almost the same fluctuation $\Delta\delta$, regardless of their energy in the trap, i.e., we consider a *homogeneous* broadening effect. We obtain the signal from many repetitions of the same experiment by integrating $w_{\text{echo}}(\Delta\delta, 2\tau_\pi)$ over all fluctuation amplitudes $\Delta\delta$, weighted by a probability distribution $p(\Delta\delta, \tau_\pi)$ which is assumed to be a Gaussian,

$$p(\Delta\delta, \tau_\pi) = \frac{1}{\sqrt{2\pi}\,\sigma(\tau_\pi)} \exp\left[-\frac{(\Delta\delta)^2}{2\sigma(\tau_\pi)^2} \right] \qquad (4)$$

with mean $\overline{\Delta\delta} = 0$ and variance $\sigma(\tau_\pi)^2$. This results in an echo visibility of $V(2\tau_\pi) = V_0 \exp[-\frac{1}{2}\tau_\pi^2 \sigma(\tau_\pi)^2]$. We found that the pointing instabilities of the dipole trap laser beams are the dominant source of irreversible dephasing. Any change of the relative position of the two interfering laser beams changes the interference contrast and hence the light shift δ_0. Position fluctuations can arise from shifts of the laser beam itself, from acoustic vibrations of the mirrors or from air flow. Other dephasing effects such as intensity and magnetic field fluctuations, elastic collisions, heating, fluctuations of the microwave power and the pulse duration were also analyzed and found to be negligible compared to the effect of the pointing instabilities.

The fluctuation of the trap depth due to pointing instabilities was measured by mutually detuning the two dipole trap beams by $\Delta\nu = 10$ MHz and overlapping them on a fast photodiode. The amplitude of the resulting beat signal directly measures the interference contrast of the two beams and is thus proportional to the depth of the potential wells of the standing wave dipole trap. We found that the relative fluctuations for time scales of $t > 100$ ms reach up to 3%. From records of the beat signal amplitude we extract the Allan variance, defined as $\tilde{\sigma}_{\text{A}}^2(\tau) = \frac{1}{m}\sum_{k=1}^{m}(\overline{x}_{\tau,k+1} - \overline{x}_{\tau,k})^2/2$, where $\overline{x}_{\tau,k}$ denotes the average of the normalized beat signal amplitude over the kth time interval τ [13]. The Allan deviation $\tilde{\sigma}_{\text{A}}(\tau_\pi)$ directly measures the difference of the detunings, averaged over τ_π, before and after the π pulse. This results in frequency fluctuations $\sigma(\tau_\pi) = \sqrt{2}\delta_0\tilde{\sigma}_{\text{A}}(\tau_\pi)$, yielding a theoretical spin-echo visibility $V^{\text{th}}(2\tau_\pi) = \exp[-\tilde{\sigma}_{\text{A}}(\tau_\pi)^2\delta_0^2\tau_\pi^2]$ which is plotted together with the measured spin-echo visibility in Fig. 1(c). The upper curves show the expected visibility in the case of well overlapped beams, whereas for the lower curves, we slightly misaligned the beams so that variations of the relative beam position cause a first order variation of the beat signal amplitude, since the beams overlap on the slopes of the Gaussian profile. Our data points lie in between these best and worst case predictions.

The population decay time, T_1, can be neglected in our experiment. It is governed by the scattering of photons from the dipole trap laser, which couples the two hyperfine ground states via a two-photon Raman transition. However, this effect is suppressed due to a destructive interference effect [5,14] causing a relaxation on a time scale of 8 s for $U_0 = 1$ mK. As a consequence, the various decay/dephasing mechanisms can be treated independently because of their different time scales ($T_2^* \ll T_2' \ll T_1$).

Finally, we demonstrate the controlled quantum state transportation of neutral atoms. We show that the atomic coherence persists while moving the atoms back and forth over macroscopic distances by shifting the standing wave dipole trap. For this purpose, we essentially perform a spin-echo measurement, with the addition that the atoms are transported between the microwave pulses. The sequence is visualized in Fig. 2. After the $\pi/2$ pulse at the MOT position, the atom is displaced by 1 mm before the π pulse is applied. The atom is then transported back to its initial position where we apply the second $\pi/2$ pulse. The corresponding spin-echo signal is shown in Fig. 3, together with a reference signal, showing a spin echo obtained without transportation. The spin echo prevails if we transport the atom between the microwave pulses, however with slightly reduced visibility; see Fig. 3(b). In these experiments, the dipole trap is lowered to $U_0 = 0.1$ mK in order to guarantee long coherence times along with high transportation efficiencies. The atoms were transported over a distance of 1 mm within 2 ms, resulting in an acceleration of $a = 1.0 \times 10^3$ m/s^2.

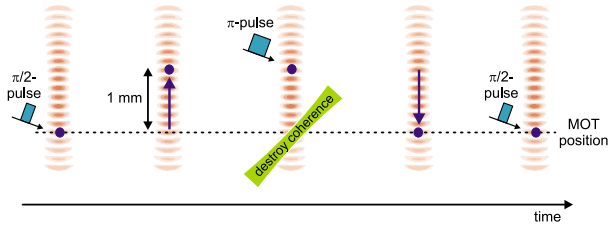

FIG. 2 (color online). Quantum state transportation. An atom prepared in a superposition of hyperfine states is displaced by 1 mm. Synchronously to the π pulse, we shine in a state mixing laser across the initial position. After transporting the atom back to its initial position, the state superposition is analyzed by means of a second $\pi/2$ pulse.

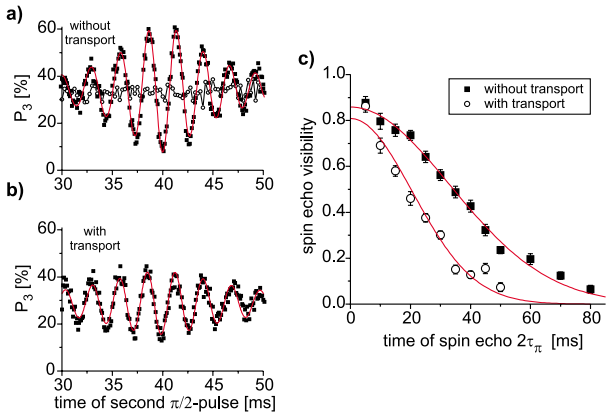

FIG. 3 (color online). Spin echo with and without transport, according to the scheme in Fig. 2. (a) Without transport, with (circles) and without mixing laser (squares); (b) atoms are transported by 1 mm, with mixing laser applied at the initial position. The lines in (a) and (b) are fits according to the analytic model presented in the text. (c) Visibility of the spin echo. The faster decay of the visibility with transport can be explained by heating of the atoms during the transportation procedure.

In order to underline that the coherence has actually been moved spatially in this experiment, we illuminate the position of the MOT with an off-resonant "state mixing laser" (detuning +30 GHz) simultaneously with the π pulse for 3 ms. The parameters of the state mixing laser, which is focused to a waist of 50 μm, are chosen such that it incoherently mixes the two hyperfine states. A scattering rate of 2 photons/ms is sufficiently high to just mix the hyperfine states but at the same time to minimize the influence on the transported atoms. Indeed the fringes disappear when the atoms are not transported. The coherence time is reduced by a factor of 2 by the transportation procedure. This can be explained by the abrupt acceleration of the potential [4]. For each of the two transports, the acceleration is first abruptly changed from zero to a, from a to $-a$ after half the transportation distance, and back to zero at the end. In order to calculate the heating effect caused by this abrupt acceleration, we assume an initial energy of $E = 0.3U_0$, calculated from the T_2^* times of the signals of Fig. 3. Numerical calculations reveal that the maximum energy gain caused by the six nonadiabatic changes of the acceleration amounts to $\Delta E = 0.15U_0$ (=150 μK). This energy gain causes a change of the average detuning $\Delta\delta$, large enough to account for the observed faster decay of the visibility of the spin echo. The existence of a heating effect is supported by the measurement of an atom survival probability with transportation of 70%, compared to 80% without transportation.

Using sodium atoms in a red detuned Nd:YAG dipole trap ($U_0 = 0.4$ mK), a dephasing time of $T_2^* = 15$ ms was reported [15], which is comparable to our observation. In the same paper, significantly longer coherence times ($T_2^* = 4$ s) were observed in blue detuned traps [15]. In other experiments, the inhomogeneous broadening has been reduced by the addition of a weak light field, spatially overlapped with the trapping laser field and whose frequency is tuned in between the two hyperfine levels [9]. Because of the different wavelengths the application of this technique is impossible in a standing wave dipole trap. Of course, cooling the atoms to the lowest vibrational level, e.g., by using Raman sideband cooling techniques, would also reduce inhomogeneous broadening.

Our experiment opens the route to the realization of a quantum shift register. Most recently, we spatially resolved single atoms in separate potential wells of the dipole trap by means of an intensified CCD camera. This fact allowed us to read out the quantum states of the trapped atoms individually. Moreover, we plan to individually address the atoms in a magnetic gradient field. Finally, the possibility of coherently transporting quantum states should allow us to let atoms interact at a location different from the preparation and readout. More specifically, our experiments aim at the deterministic transport of two or more atoms into an optical high finesse resonator, where they could controllably interact via photon exchange. This should enable us to entangle neutral atoms [16] or to realize quantum gates [17]. This Letter demonstrates that in these experiments state preparation and detection, as well as quantum state rotations, can now take place outside the cavity.

This work was supported by the Deutsche Forschungsgemeinschaft and the EC.

*Electronic address: kuhr@iap.uni-bonn.de

[1] D. Kielpinski, C. Monroe, and D. J. Wineland, Nature (London) **417**, 709 (2002).
[2] M. Rowe *et al.*, Quantum Inf. Comp. **2**, 257 (2002).
[3] S. Kuhr *et al.*, Science **293**, 278 (2001).
[4] D. Schrader *et al.*, Appl. Phys. B **73**, 819 (2001).
[5] D. Frese *et al.*, Phys. Rev. Lett. **85**, 3777 (2000).
[6] S. Kuhr *et al.* (to be published).
[7] N. Ramsey, *Molecular Beams* (Oxford University Press, London, 1956).
[8] L. Allen and J. H. Eberly, *Optical Resonance and Two-Level Atoms* (Wiley, New York, 1975).
[9] A. Kaplan, M. F. Andersen, and N. Davidson, Phys. Rev. A **66**, 045401 (2002).
[10] W. Alt *et al.*, Phys. Rev. A **67**, 033403 (2003).
[11] E. Hahn, Phys. Rev. **80**, 580 (1950).
[12] M. F. Andersen, A. Kaplan, and N. Davidson, Phys. Rev. Lett. **90**, 023001 (2003).
[13] D. W. Allan, Proc. IEEE **54**, 221 (1966).
[14] R. A. Cline, J. D. Miller, M. R. Matthews, and D. J. Heinzen, Opt. Lett. **19**, 207 (1994).
[15] N. Davidson, H. J. Lee, C. S. Adams, M. Kasevich, and S. Chu, Phys. Rev. Lett. **74**, 1311 (1995).
[16] S.-B. Zheng and G.-C. Guo, Phys. Rev. Lett. **85**, 2392 (2000).
[17] T. Pellizzari, S. A. Gardiner, J. I. Cirac, and P. Zoller, Phys. Rev. Lett. **75**, 3788 (1995).